

# Measuring nonadiabaticity of molecular quantum dynamics with quantum fidelity and with its efficient semiclassical approximation

Tomáš Zimmermann and Jiří Vaníček\*

*Laboratory of Theoretical Physical Chemistry, Institut des Sciences et Ingénierie Chimiques, Ecole Polytechnique Fédérale de Lausanne (EPFL), CH-1015, Lausanne, Switzerland*

We propose to measure nonadiabaticity of molecular quantum dynamics rigorously with the quantum fidelity between the Born-Oppenheimer and fully nonadiabatic dynamics. It is shown that this measure of nonadiabaticity applies in situations where other criteria, such as the energy gap criterion or the extent of population transfer, fail. We further propose to estimate this quantum fidelity efficiently with a generalization of the dephasing representation to multiple surfaces. Two variants of the multiple-surface dephasing representation (MSDR) are introduced, in which the nuclei are propagated either with the fewest-switches surface hopping (FSSH) or with the locally mean field dynamics (LMFD). The LMFD can be interpreted as the Ehrenfest dynamics of an ensemble of nuclear trajectories, and has been used previously in the nonadiabatic semiclassical initial value representation. In addition to propagating an ensemble of classical trajectories, the MSDR requires evaluating nonadiabatic couplings and solving the Schrödinger (or more generally, the quantum Liouville-von Neumann) equation for a single discrete degree of freedom. The MSDR can be also used to measure the importance of other terms present in the molecular Hamiltonian, such as diabatic couplings, spin-orbit couplings, or couplings to external fields, and to evaluate the accuracy of quantum dynamics with an approximate nonadiabatic Hamiltonian. The method is tested on three model problems introduced by Tully, on a two-surface model of dissociation of NaI, and a three-surface model including spin-orbit interactions. An example is presented that demonstrates the importance of often-neglected second-order nonadiabatic couplings.

## I. INTRODUCTION

Nonadiabatic effects give rise to a great variety of phenomena in chemical dynamics.<sup>1-3</sup> To account for these effects, many theoretical methods have been developed. The most accurate but also the most computationally demanding are wave packet approaches which solve the Schrödinger equation for both electrons and nuclei directly. Some wave packet methods, e.g., the multi-configuration time-dependent Hartree method,<sup>4,5</sup> have been successfully applied to problems with tens of degrees of freedom. Trajectory based nonadiabatic Bohmian dynamics<sup>6,7</sup> is another in principle exact method, which can be, moreover, combined with electronic structure computed on the fly.<sup>8</sup> Less accurate but also less expensive are various semiclassical approaches, which can also describe some quantum effects, especially on the nuclear motion. These include multiple-spawning methods,<sup>9,10</sup> methods based on the Herman-Kluk propagator,<sup>11-14</sup> or the surface hopping and jumping method of Heller *et al.*<sup>15</sup> The most widely used are methods in which the nuclei are treated classically and the quantum effects enter only through interaction with electrons, which are described quantum mechanically. Among these belong methods based directly on the mixed quantum-classical Liouville equation,<sup>16-24</sup> the mean field Ehrenfest dynamics, various surface hopping methods,<sup>25-27</sup> or methods in which the classical limit is obtained by linearizing the path integral representation of the quantum propagator.<sup>28</sup>

Unfortunately, all of these methods are significantly more computationally demanding than their adiabatic or diabatic counterparts. (In the following, we discuss mostly nonadiabatic dynamics. Nevertheless, the discus-

sion holds almost entirely also for the nonadiabatic dynamics in the diabatic basis.) One goal of this paper is to find a general criterion which would determine when a given dynamics is nonadiabatic enough to justify the use of the expensive nonadiabatic methods. Several possible criteria could be envisaged. One widely used criterion is the extent of population transfer or, more precisely, the decay of survival probability  $P_{QM}$  on the initially populated potential energy surface (PES) due to nonadiabatic couplings. Although a fast decay of  $P_{QM}$  is a clear sign of nonadiabaticity of the dynamics, the opposite implication is not necessarily true, as can be seen in Ref. 29 and as will also be demonstrated below. Another criterion, often employed to decide when to “switch on” the couplings in nonadiabatic calculations,<sup>30</sup> is the energy gap criterion: one simply monitors the energy difference between PESs and when it becomes sufficiently small, the dynamics is considered nonadiabatic. While useful in practical calculations, this criterion does not always reflect the actual extent of nonadiabaticity, which also depends on nonadiabatic couplings and on the nuclear momentum. Other approximate criteria, which are intermediate between the two criteria mentioned, estimate the change of  $P_{QM}$  from basic properties of the PESs, from couplings between the PESs, and from the nuclear velocity. Examples include variants<sup>31</sup> of the Landau-Zener-Stückelberg model.<sup>32-36</sup>

In Ref. 29 we proposed a more rigorous quantitative criterion of the non(a)diabaticity of the quantum dynamics, based on the quantum fidelity  $F_{QM}$ <sup>37</sup> between the adiabatically and nonadiabatically propagated molecular wave functions. More precisely,

$$F_{QM}(t) = |f_{QM}(t)|^2 = |\langle \psi^0(t) | \psi^\epsilon(t) \rangle|^2, \quad (1)$$

where  $|\psi^0(t)\rangle$  is the quantum state of the molecule evolved using the adiabatic Hamiltonian  $\hat{H}^0$  with uncoupled PESs and  $|\psi^\epsilon(t)\rangle$  is the quantum state evolved using the fully coupled nonadiabatic Hamiltonian  $\hat{H}^\epsilon$ . When  $F_{\text{QM}} \approx 1$ ,  $|\psi^0(t)\rangle$  is close to  $|\psi^\epsilon(t)\rangle$  and an adiabatic simulation is a good approximation to the nonadiabatic simulation. When  $F_{\text{QM}} \ll 1$ , adiabatic treatment is inadequate and a nonadiabatic method should be used. Unlike the energy gap and population transfer criteria, the fidelity criterion can detect more subtle nonadiabatic effects caused, e.g., by the displacement and/or interference on a single PES surface (see Fig. 1). Panels (c) and (d) of Fig. 1 show two extreme examples in which the nonadiabatic couplings induce a hop to the excited surface followed by a hop back to the ground surface so that at large times, only the ground state is occupied. While the nonadiabatic couplings have no effect on the survival probability on the ground surface, they have a large effect on the molecular wavefunction since the returning wavepacket may accumulate a time delay (panel c) or a phase (panel d), and hence can have a zero overlap with the wavepacket propagated adiabatically. Although neither case can be detected by the survival probability criterion, both scenarios can be detected easily by fidelity (1).

Due to the generality of definition (1), fidelity can be employed in many applications with nonadiabatic dynamics, depending on the choice of  $\hat{H}^0$  and  $\hat{H}^\epsilon$ . Very recently, this fidelity criterion of nonadiabaticity was used to find the optimal time-dependent Hamiltonian maximizing the adiabaticity of the dynamics from an initial state to a desired target state.<sup>38</sup> Besides the use of fidelity to measure nonadiabaticity, two other applications are explored here. First, we consider the importance of additional terms in a nonadiabatic Hamiltonian, such as spin-orbit coupling terms or couplings to an external field. In this case, both  $\hat{H}^0$  and  $\hat{H}^\epsilon$  are coupled by nonadiabatic coupling terms, and the additional term of interest, missing in  $\hat{H}^0$ , is present in  $\hat{H}^\epsilon$ . Second,  $F_{\text{QM}}$  may be used to evaluate quantitatively the accuracy of the quantum dynamics with an approximate or interpolated nonadiabatic Hamiltonian  $\hat{H}^0$  in comparison to the quantum dynamics with an accurate nonadiabatic Hamiltonian  $\hat{H}^\epsilon$ . This application is a generalization to nonadiabatic dynamics of the idea proposed for adiabatic dynamics in Refs. 39 and 40.

The remaining (but difficult) question is how to compute  $F_{\text{QM}}$ . The most straightforward way would be to propagate the wave functions with some wave packet method and to use Eq. (1) directly. This approach, however, suffers from the previously mentioned disadvantages of wave packet methods. Instead, below we derive an accurate, yet efficient semiclassical method capable of computing not only fidelity  $F_{\text{QM}}$  but also fidelity amplitude  $f_{\text{QM}}$ . The method, which we refer to as *multiple-surface dephasing representation* (MSDR), is a generalization of the dephasing representation (DR),<sup>41–43</sup> derived for the adiabatic dynamics using the Van Vleck

propagator. In the single surface setting, the DR is closely related to the semiclassical perturbation approximation of Hubbard and Miller<sup>44</sup> and phase averaging of Mukamel.<sup>45</sup> Its main applications include calculations of electronic spectra<sup>45–50</sup> and evaluations of stability of quantum dynamics.<sup>42,43,51–53</sup> The main advantage of the MSDR compared to wave packet methods is that the computational cost of MSDR, similarly to the DR, does not scale exponentially with the number of degrees of freedom.<sup>54</sup> The MSDR can therefore be applied to problems with dimensionality far beyond the scope of current methods of quantum dynamics. The advantage of MSDR in comparison to most other semiclassical approaches is that the MSDR does not require the Hessian of the potential energy, which is often the most expensive part of semiclassical calculations (see, e.g., Ref. 55). Finally, in contrast to methods treating the motion of nuclei completely classically, the MSDR includes some nuclear quantum effects approximately via the interference between the classical trajectories representing a wave packet.

The MSDR is not the first extension of the DR to nonadiabatic dynamics. In Ref. 29 we have introduced another extension of the DR, which is here referred to as *integral multiple-surface dephasing representation* (IMSDR) and which performs satisfactorily in the case of nearly diabatic dynamics in the diabatic basis. Unfortunately, the accuracy of the IMSDR deteriorates when the dynamics is far from the diabatic limit. Another important limitation of the IMSDR is that it cannot be used in the adiabatic basis. Below we shall demonstrate that the MSDR is both more accurate and more general than the IMSDR. A small price to pay for this improvement is that in contrast to the IMSDR, in which fidelity is computed as an interference integral at the end of dynamics, in the MSDR the Liouville-Von Neumann equation for one discrete (collective electronic) degree of freedom has to be solved during the dynamics. For pure states, this equation is simple and is equivalent to the Schrödinger equation for one discrete degree of freedom which is already solved during the Ehrenfest or fewest switches surface hopping (FSSH) dynamics. Both MSDR and IMSDR reduce to the original DR for systems with a single PES.

The outline of the paper is as follows: in Section II, the MSDR is derived. In Section III, the method is used to evaluate nonadiabaticity and nonadiabaticity of quantum dynamics in model cases, to evaluate the importance of an additional coupling term in a nonadiabatic Hamiltonian and to evaluate the accuracy of an approximate Hamiltonian. Computational details are summarized in the same section. Section IV concludes the paper.

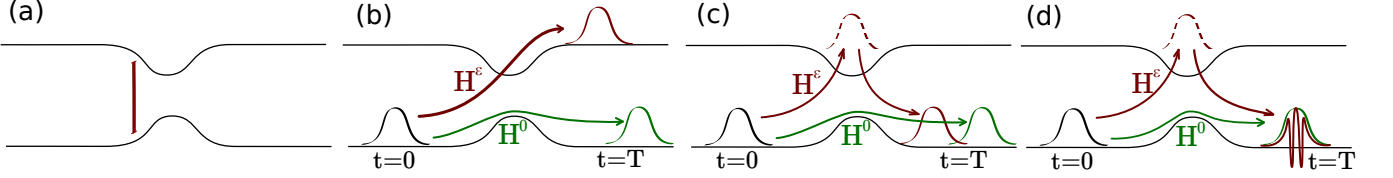


Figure 1. Possible criteria of non(a)diabaticity of quantum dynamics. The static energy-gap criterion does not take into account the dynamics of the wave packet (a). The population transfer criterion measures the actual decay of probability density on the initial PES (b). It is more sensitive than the static energy-gap criterion. Fidelity criterion can capture the population transfer (b) as well as other nonadiabatic effects such as displacement (c) or interference (d) on a single PES, which would be undetected by the population transfer criterion.  $\hat{\mathbf{H}}^0$  is the decoupled Born-Oppenheimer Hamiltonian, whereas  $\hat{\mathbf{H}}^\epsilon$  is the fully coupled nonadiabatic Hamiltonian.

## II. THEORY

### A. MSDR

A starting point for the derivation of the MSDR is the expression for quantum fidelity amplitude formulated in terms of the density matrix<sup>43</sup>

$$f_{\text{QM}}(t) = \text{Tr} \left( e^{-i\hat{\mathbf{H}}^\epsilon t/\hbar} \cdot \hat{\rho}^{\text{init}} \cdot e^{+i\hat{\mathbf{H}}^0 t/\hbar} \right), \quad (2)$$

where  $\hat{\rho}^{\text{init}}$  is the density operator of the initial state,  $\hat{\mathbf{H}}^0$  and  $\hat{\mathbf{H}}^\epsilon$  are two different molecular Hamiltonians expressed either in the diabatic or adiabatic basis. (**Bold** face denotes  $n \times n$  matrices acting on the Hilbert space spanned by  $n$  electronic states, hat denotes nuclear operators.) Note that Eq. (2) applies to both pure and mixed states.<sup>43</sup> Formally,  $\hat{\mathbf{H}}^\epsilon$  can be written as  $\hat{\mathbf{H}}^\epsilon = \hat{\mathbf{H}}^0 + \epsilon \hat{\mathbf{V}}$ , where  $\epsilon$  controls the extent of the perturbation. Expressing  $f_{\text{QM}}$  in the interaction picture gives

$$f_{\text{QM}}(t) = \text{Tr} \left( \hat{\rho}^{\text{init}} \cdot \hat{\mathbf{E}}(t) \right), \quad (3)$$

where

$$\hat{\mathbf{E}}(t) := e^{+i\hat{\mathbf{H}}^0 t/\hbar} \cdot e^{-i\hat{\mathbf{H}}^\epsilon t/\hbar} = \mathcal{T} e^{-i\epsilon \int_0^t \hat{\mathbf{V}}^I(t') dt'/\hbar} \quad (4)$$

is the echo operator<sup>51,56</sup> and

$$\hat{\mathbf{V}}^I(t) = e^{i\hat{\mathbf{H}}^0 t/\hbar} \cdot \hat{\mathbf{V}} \cdot e^{-i\hat{\mathbf{H}}^0 t/\hbar} \quad (5)$$

is the perturbation in the interaction picture. A partial Wigner transform<sup>57</sup> of Eq. (3) over nuclear degrees of freedom yields an alternative exact expression for the fidelity amplitude,

$$f_{\text{QM}}(t) = h^{-D} \text{Tr}_e \int dX \rho_{\text{W}}^{\text{init}}(X) \cdot \mathbf{E}_{\text{W}}(X, t), \quad (6)$$

where  $\mathbf{A}_{\text{W}}(X)$  is the partial Wigner transform of operator  $\hat{\mathbf{A}}$ ,

$$\mathbf{A}_{\text{W}}(X) = \int d\xi \left\langle Q - \frac{\xi}{2} \left| \hat{\mathbf{A}} \left| Q + \frac{\xi}{2} \right. \right. \right\rangle \exp \left( i \frac{\xi \cdot P}{\hbar} \right), \quad (7)$$

$X$  denotes the point  $(Q, P)$  in the  $2D$ -dimensional phase space, and  $\text{Tr}_e$  is the trace over electronic degrees of freedom. Direct evaluation of the Wigner transform of the echo operator is unfortunately difficult without approximations. As the first approximation, one may truncate the Taylor expansion of the exponential operator in the Wigner transform of a product of two operators

$$\begin{aligned} (\hat{\mathbf{A}} \cdot \hat{\mathbf{B}})_{\text{W}} &= \exp \left( \frac{i\hbar}{2} \{.,.\} \right) (\mathbf{A}_{\text{W}}, \mathbf{B}_{\text{W}}) \\ &= \mathbf{A}_{\text{W}} \exp \left[ \frac{i\hbar}{2} \left( \overleftarrow{\frac{\partial}{\partial Q}} \overrightarrow{\frac{\partial}{\partial P}} - \overleftarrow{\frac{\partial}{\partial P}} \overrightarrow{\frac{\partial}{\partial Q}} \right) \right] \mathbf{B}_{\text{W}} \end{aligned} \quad (8)$$

after the zeroth-order term. In Eq. (8),  $\{\mathbf{A}, \mathbf{B}\} = \frac{\partial \mathbf{A}}{\partial Q} \cdot \frac{\partial \mathbf{B}}{\partial P} - \frac{\partial \mathbf{A}}{\partial P} \cdot \frac{\partial \mathbf{B}}{\partial Q}$  is the Poisson bracket over the nuclear degrees of freedom and arrows indicate on which argument the derivatives act. An iterative application of expansion (8) to the echo operator (4) expressed as a time-ordered product of the short time propagators gives

$$\left( \mathcal{T} e^{-i\epsilon \int_0^t \hat{\mathbf{V}}^I(t') dt'/\hbar} \right)_{\text{W}} \simeq \mathcal{T} e^{-i\epsilon \int_0^t \mathbf{V}_{\text{W}}^I(X, t') dt'/\hbar}. \quad (9)$$

To evaluate this expression, the time evolution of  $\mathbf{V}_{\text{W}}^I(X, t)$  is required. The second approximation involves replacing the exact equation of motion by a mixed quantum-classical (MQC) propagation scheme described below, leading to the final expression for MSDR of fidelity amplitude,

$$\begin{aligned} f_{\text{MSDR}}(t) &= h^{-D} \text{Tr}_e \int dX \rho_{\text{W}}^{\text{init}}(X) \cdot \mathcal{T} e^{-i\epsilon \int_0^t \mathbf{V}_{\text{W}, \text{MQC}}^I(X, t') dt'/\hbar} \\ &= \left\langle \mathcal{T} e^{-i\epsilon \int_0^t \mathbf{V}_{\text{W}, \text{MQC}}^I(X, t') dt'/\hbar} \right\rangle_{\rho_{\text{W}}^{\text{init}}(X)}, \end{aligned} \quad (10)$$

where the average in the last row is defined in general as

$$\langle \mathbf{A}(X) \rangle_{\rho(X)} := \frac{\text{Tr}_e \int dX \rho(X) \cdot \mathbf{A}(X)}{\text{Tr}_e \int dX \rho(X)}.$$

Equation (10) makes it clear that the only fundamental difference between the MSDR and IMSDR introduced in Ref. 29 is the time ordering operator  $\mathcal{T}$  present in the MSDR but missing in the IMSDR.

## B. Propagation scheme

Equation (10) gives  $f_{\text{MSDR}}$  in terms of  $\mathbf{V}_{\text{W,MQC}}^{\text{I}}(X, t)$ ; what remains to be done is finding a prescription for  $\mathbf{V}_{\text{W,MQC}}^{\text{I}}(X, t)$ . The exact equation of motion for  $\mathbf{V}_{\text{W}}^{\text{I}}(X, t)$  in the interaction picture is

$$\frac{\partial \mathbf{V}_{\text{W}}^{\text{I}}(X, t)}{\partial t} = \frac{i}{\hbar} \left[ \hat{\mathbf{H}}^0, \hat{\mathbf{V}}^{\text{I}}(t) \right]_{\text{W}}(X). \quad (11)$$

Note that Eq. (11) is, up to the sign, the same as the partially Wigner transformed Liouville-Von Neumann equation describing the propagation of the density matrix of the unperturbed system:

$$\frac{\partial \rho_{\text{W}}(X, t)}{\partial t} = -\frac{i}{\hbar} \left[ \hat{\mathbf{H}}^0, \hat{\rho}(t) \right]_{\text{W}}(X). \quad (12)$$

We will take advantage of this analogy and derive our approximate propagation scheme from Eq. (12) instead of from Eq. (11). This will turn out to be slightly easier and, more importantly, we will simultaneously find an approximate solution of a much more general problem of propagating the density matrix. Below we omit superscript 0 in  $\hat{\mathbf{H}}^0$  since now we deal with a single Hamiltonian. In the system consisting of light electrons and heavy nuclei, Eq. (12) is approximated to the first order in the mass ratio  $\sqrt{\frac{m}{M}}$  by the mixed quantum-classical Liouville equation<sup>17,58–63</sup>

$$\begin{aligned} \frac{\partial \rho_{\text{W,MQC}}}{\partial t} = & -\frac{i}{\hbar} [\mathbf{H}_{\text{W}}, \rho_{\text{W,MQC}}] \\ & + \frac{1}{2} (\{ \mathbf{H}_{\text{W}}, \rho_{\text{W,MQC}} \} - \{ \rho_{\text{W,MQC}}, \mathbf{H}_{\text{W}} \}), \end{aligned} \quad (13)$$

where the explicit dependence of  $\rho_{\text{W,MQC}}$  on time and on the nuclear phase space coordinate  $X$  was omitted for clarity.

Equation (10) together with Eq. (13) define the MSDR. Several numerical approaches exist that solve Eq. (13) in terms of ‘‘classical’’ trajectories  $X(t)$ . However, since trajectory based methods for solving Eq. (13) are still relatively complicated, below we study two variants of MSDR where Eq. (13) is further approximated. The common feature of the two approximations is that all elements of  $\rho_{\text{W}}(X, t)$  are propagated using the same PES (which may, nevertheless, differ for different trajectories). For simplicity, from now on the subscript MQC is omitted.

### 1. Locally mean field dynamics

The first approach starts by rewriting  $\rho_{\text{W}}(X, t)$  as

$$\rho_{\text{W}}(X, t) = \rho(X, t) \rho_e(X, t), \quad (14)$$

where  $\rho(X, t) := \text{Tr}_e \rho_{\text{W}}(X, t)$  is a scalar function of  $X$  and  $t$  and hence  $\text{Tr}_e \rho_e(X, t) = 1$  for all  $X$  and  $t$ . By

substituting the still exact ansatz (14) into Eq. (13), one obtains

$$\begin{aligned} \frac{\partial \rho}{\partial t} \rho_e + \rho \frac{\partial \rho_e}{\partial t} = & -\frac{i}{\hbar} \rho [\mathbf{H}_{\text{W}}, \rho_e] \\ & + \frac{1}{2} \frac{\partial \rho}{\partial P} \left[ \frac{\partial \mathbf{H}_{\text{W}}}{\partial Q}, \rho_e \right]_+ \\ & + \frac{1}{2} \rho \left[ \frac{\partial \mathbf{H}_{\text{W}}}{\partial Q}, \frac{\partial \rho_e}{\partial P} \right]_+ \\ & - \frac{1}{2} \frac{\partial \rho}{\partial Q} \left[ \frac{\partial \mathbf{H}_{\text{W}}}{\partial P}, \rho_e \right]_+ \\ & - \frac{1}{2} \rho \left[ \frac{\partial \mathbf{H}_{\text{W}}}{\partial P}, \frac{\partial \rho_e}{\partial Q} \right]_+, \end{aligned} \quad (15)$$

where  $[\mathbf{A}, \mathbf{B}]_+ = \mathbf{A} \cdot \mathbf{B} + \mathbf{B} \cdot \mathbf{A}$  is the anticommutator. In the next step, the trace over the electronic degrees of freedom is performed, which in the diabatic basis leads to the following equation of motion for  $\rho(X, t)$ :

$$\begin{aligned} \frac{\partial \rho}{\partial t} = & \frac{\partial \rho}{\partial P} \left\langle \frac{\partial \mathbf{H}_{\text{W}}}{\partial Q} \right\rangle_e - \frac{\partial \rho}{\partial Q} \left\langle \frac{\partial \mathbf{H}_{\text{W}}}{\partial P} \right\rangle_e \\ & + \rho \text{Tr}_e \left( \frac{\partial \mathbf{H}_{\text{W}}}{\partial Q} \cdot \frac{\partial \rho_e}{\partial P} \right), \end{aligned} \quad (16)$$

where  $\langle \mathbf{A} \rangle_e = \text{Tr}_e(\rho_e \cdot \mathbf{A})$  is a partial average of  $\mathbf{A}$  over the electronic subspace and where we have used that  $\text{Tr}_e \left( \frac{\partial \mathbf{H}_{\text{W}}}{\partial P} \cdot \frac{\partial \rho_e}{\partial Q} \right) = \frac{P}{M} \text{Tr}_e \left( \frac{\partial \rho_e}{\partial Q} \right) = 0$ . (The equation of motion in the adiabatic basis will be derived later.) Substitution of Eq. (16) back into Eq. (15) yields

$$\begin{aligned} \rho \frac{\partial \rho_e}{\partial t} = & -\frac{i}{\hbar} \rho [\mathbf{H}_{\text{W}}, \rho_e] \\ & + \frac{\partial \rho}{\partial P} \left( \frac{1}{2} \left[ \frac{\partial \mathbf{H}_{\text{W}}}{\partial Q}, \rho_e \right]_+ - \left\langle \frac{\partial \mathbf{H}_{\text{W}}}{\partial Q} \right\rangle_e \cdot \rho_e \right) \\ & + \frac{1}{2} \rho \left[ \frac{\partial \mathbf{H}_{\text{W}}}{\partial Q}, \frac{\partial \rho_e}{\partial P} \right]_+ \\ & - \frac{\partial \rho}{\partial Q} \left( \frac{1}{2} \left[ \frac{\partial \mathbf{H}_{\text{W}}}{\partial P}, \rho_e \right]_+ - \left\langle \frac{\partial \mathbf{H}_{\text{W}}}{\partial P} \right\rangle_e \cdot \rho_e \right) \\ & - \rho \left\langle \frac{\partial \mathbf{H}_{\text{W}}}{\partial P} \right\rangle_e \cdot \frac{\partial \rho_e}{\partial Q} \\ & - \rho \rho_e \text{Tr} \left( \frac{\partial \mathbf{H}_{\text{W}}}{\partial Q} \cdot \frac{\partial \rho_e}{\partial P} \right), \end{aligned} \quad (17)$$

where identity  $\frac{1}{2} \left[ \frac{\partial \mathbf{H}_{\text{W}}}{\partial P}, \frac{\partial \rho_e}{\partial Q} \right]_+ = \frac{P}{M} \frac{\partial \rho_e}{\partial Q} = \left\langle \frac{\partial \mathbf{H}_{\text{W}}}{\partial P} \right\rangle_e \cdot \frac{\partial \rho_e}{\partial Q}$  was used in the fifth row. Both Eqs. (16) and (17) contain terms of the form  $\left\langle \frac{\partial \mathbf{H}_{\text{W}}}{\partial P} \right\rangle_e \frac{\partial f}{\partial Q}$  and  $\left\langle \frac{\partial \mathbf{H}_{\text{W}}}{\partial Q} \right\rangle_e \frac{\partial f}{\partial P}$ , which can be combined with the time derivative  $\frac{\partial f}{\partial t}$  to form the convective derivative

$$\frac{Df}{Dt} = \frac{\partial f}{\partial t} + \dot{Q} \frac{\partial f}{\partial Q} + \dot{P} \frac{\partial f}{\partial P}$$

and transform the equations from the Eulerian reference frame at rest to the Lagrangian reference frame moving with the phase space flow given by the vector field

$$\left(\dot{Q}, \dot{P}\right) = \left(\left\langle \frac{\partial \mathbf{H}_W}{\partial P} \right\rangle_e, -\left\langle \frac{\partial \mathbf{H}_W}{\partial Q} \right\rangle_e\right). \quad (18)$$

In the Lagrangian frame, Eq. (16) transforms to

$$\frac{D\rho}{Dt} = \rho \text{Tr}_e \left( \frac{\partial \mathbf{H}_W}{\partial Q} \cdot \frac{\partial \rho_e}{\partial P} \right). \quad (19)$$

Since the two terms in the fourth row of Eq. (17) cancel each other exactly, this equation transforms to

$$\begin{aligned} \frac{D\rho_e}{Dt} = & -\frac{i}{\hbar} [\mathbf{H}_W, \rho_e] \\ & + \frac{1}{\rho} \frac{\partial \rho}{\partial P} \left( \frac{1}{2} \left[ \frac{\partial \mathbf{H}_W}{\partial Q}, \rho_e \right]_+ - \left\langle \frac{\partial \mathbf{H}_W}{\partial Q} \right\rangle_e \rho_e \right) \\ & + \left( \frac{1}{2} \left[ \frac{\partial \mathbf{H}_W}{\partial Q}, \frac{\partial \rho_e}{\partial P} \right]_+ - \left\langle \frac{\partial \mathbf{H}_W}{\partial Q} \right\rangle_e \cdot \frac{\partial \rho_e}{\partial P} \right) \\ & - \rho_e \text{Tr}_e \left( \frac{\partial \mathbf{H}_W}{\partial Q} \cdot \frac{\partial \rho_e}{\partial P} \right). \end{aligned} \quad (20)$$

Note that the second and third row of the right hand side of Eq. (20) contain differences (put in parentheses for emphasis) between products of the electronic density matrix (or its  $P$  derivative) with the nonaveraged and averaged gradients of the Hamiltonian. Therefore, the second and third row may often be small compared to the first and fourth row of Eq. (20). The last term on the right hand side of Eq. (20) corresponds to the right hand side of Eq. (19) and is responsible for maintaining  $\text{Tr}_e \rho_e(X, t) = 1$  during the (non-approximated) MQC dynamics. Until now all operations have been exact and Eqs. (19) and (20) are equivalent to the original mixed quantum classical Liouville equation (13).

Now we will make the locally mean field approximation: Specifically, once in the Lagrangian reference frame, all terms in both Eqs. (19) and (20) containing phase space derivatives of  $\rho(X, t)$  or  $\rho_e(X, t)$  are neglected to obtain the approximate locally mean-field equations of motion. The resulting equation for  $\rho(X, t)$  in the Lagrangian reference frame is simply

$$\frac{D\rho_{\text{LMFD}}}{Dt} = 0, \quad (21)$$

and the equation of motion for the electronic part of the density matrix  $\rho_e(X, t)$  is

$$\frac{D\rho_{e,\text{LMFD}}}{Dt} = -\frac{i}{\hbar} [\mathbf{H}_W, \rho_{e,\text{LMFD}}]. \quad (22)$$

Both equations can be combined together and transformed back to the Eulerian reference frame to yield the

equation of motion for the total density matrix  $\rho_W(X, t)$ ,

$$\begin{aligned} \frac{\partial \rho_{W,\text{LMFD}}}{\partial t} = & -\frac{i}{\hbar} [\mathbf{H}_W, \rho_{W,\text{LMFD}}] \\ & + \frac{\partial \rho_{W,\text{LMFD}}}{\partial P} \left\langle \frac{\partial \mathbf{H}_W}{\partial Q} \right\rangle_e \\ & - \frac{\partial \rho_{W,\text{LMFD}}}{\partial Q} \frac{P}{M}, \end{aligned} \quad (23)$$

where we have used that  $\left\langle \frac{\partial \mathbf{H}_W}{\partial P} \right\rangle_e = \frac{P}{M}$ .

We call the dynamics expressed by Eq. (23) [or, equivalently, by Eqs. (18), (21) and (22)] the *locally mean field dynamics* (LMFD) since the force acting on nuclei at position  $X$  is the force averaged over the “electronic” part of the density matrix  $\rho_e(X, t)$  at  $X$ . Note that the well-known *Ehrenfest dynamics* (which uses a single nuclear trajectory) can be derived in a similar way using an approximate ansatz  $\rho_W^{\text{ED}} = \delta(X - X(t))\rho_e(t)$ , where  $\delta$  is the Dirac delta distribution and  $X(t)$  is the phase space coordinate at time  $t$ .<sup>64</sup> Similarly, a truly *mean field dynamics* for a wave packet different from a  $\delta$  distribution can be derived using an (again approximate) ansatz in the form of a Hartree product  $\rho_W^{\text{MFD}}(X, t) = \rho(X, t)\rho_e(t)$ .

As can be seen from Eq. (23), for pure states, each phase space point is propagated by the mean field Ehrenfest dynamics, according to Eq. (18). Nevertheless, in contrast to the purely mean field dynamics, Eq. (23) describes the propagation of the density  $\rho_W(X, t)$  using different values of  $\left\langle \frac{\partial \mathbf{H}_W}{\partial Q} \right\rangle_e$  and  $\left\langle \frac{\partial \mathbf{H}_W}{\partial P} \right\rangle_e$  for each value of  $X$ . Interestingly, this dynamics corresponds exactly to the nuclear dynamics appearing in the nonadiabatic IVR model,<sup>14,65</sup> which uses the Meyer-Miller-Stock-Thoss Hamiltonian.<sup>66,67</sup> Also note that outside of coupling regions and when only one surface is occupied, resulting trajectories are equivalent to those obtained with the Born-Oppenheimer dynamics.

To derive a corresponding LMFD equation of motion in the adiabatic basis, one can express the mixed quantum classical Liouville equation (13) in the adiabatic basis,<sup>17</sup> use the exact ansatz (14), and apply a similar LMFD approximation as above. However, this procedure is quite tedious in the adiabatic basis. The LMFD in adiabatic basis can be obtained more easily by directly transforming the final LMFD equation of motion (21) from diabatic to adiabatic basis using the relations<sup>17</sup>

$$\left( \frac{\partial \mathbf{A}_W}{\partial Q} \right)^{\text{A}} = \frac{\partial \mathbf{A}_W^{\text{A}}}{\partial Q} - [\mathbf{A}_W^{\text{A}}, \mathbf{F}] \quad \text{and} \quad (24)$$

$$\left( \frac{\partial \mathbf{A}_W}{\partial P} \right)^{\text{A}} = \frac{\partial \mathbf{A}_W^{\text{A}}}{\partial P}, \quad (25)$$

where the superscript A denotes the transformation to the adiabatic basis and  $\mathbf{F}$  is the vector matrix of nonadiabatic coupling vectors. Specifically,  $\mathbf{A}_W^{\text{A}}(X, t)$  is a matrix obtained by first partially Wigner transforming a general operator  $\mathbf{A}(t)$  [to form  $\mathbf{A}_W(X, t)$ ] and then by transforming  $\mathbf{A}_W(X, t)$  into the adiabatic basis. Matrix  $\mathbf{F}$  is

defined componentwise by  $F_{jk}(Q) = \langle \alpha_j(Q) | \frac{\partial}{\partial Q} \alpha_k(Q) \rangle$ , where  $|\alpha_k(Q)\rangle$  is  $k$ -th element of the adiabatic basis at position  $Q$ . Applying relations (24) and (25) to derivatives of both  $\mathbf{H}_W$  and  $\rho_{W,\text{LMFD}}$  in Eq. (23) immediately yields the LMFD equation of motion in the adiabatic basis,

$$\begin{aligned} \frac{\partial \rho_{W,\text{LMFD}}^A}{\partial t} = & -\frac{i}{\hbar} \left[ \mathbf{H}_W^A(X) - i\hbar \frac{P}{M} \mathbf{F}(Q), \rho_{W,\text{LMFD}}^A \right] \\ & + \frac{\partial \rho_{W,\text{LMFD}}^A}{\partial P} \cdot \left( \left\langle \frac{\partial \mathbf{H}_W^A}{\partial Q} \right\rangle_e - \langle [\mathbf{H}_W^A, \mathbf{F}] \rangle_e \right) \\ & - \frac{\partial \rho_{W,\text{LMFD}}^A}{\partial Q} \frac{P}{M}, \end{aligned} \quad (26)$$

where  $\mathbf{H}_W^A$  is the diabatic Hamiltonian matrix  $\mathbf{H}_W$  expressed in the adiabatic basis. Note that  $\mathbf{H}_W^A$  consists only of the kinetic energy term and the diagonal adiabatic potential energy matrix; in particular,  $\mathbf{H}_W^A$  does not contain the nonadiabatic couplings. Again, the dynamics of a single trajectory is identical to the Ehrenfest dynamics.

## 2. Fewest switches surface hopping

The second alternative approximate propagation scheme is based on the physically motivated FSSH algorithm.<sup>25</sup> In this scheme, each phase space point representing the Wigner density distribution is propagated independently using the FSSH dynamics. Compared to the LMFD, the FSSH is used at no additional cost, except for the stochastic hopping algorithm itself, because the same Eq. (22) (or its equivalent in the adiabatic basis) has to be solved during the electronic part of the dynamics. On the other hand, averaging the force over electronic states is avoided in the FSSH. As will be shown below, neither method is universally optimal and the best propagation method depends on a problem studied.

## C. Algorithm

### 1. General initial state

To compute  $f_{\text{MSDR}}(t)$ , we rewrite the initial density matrix exactly in the form

$$\rho_W^{\text{init}}(X) = \rho^{\text{init}}(X) \rho_e^{\text{init}}(X), \quad (27)$$

where  $\rho^{\text{init}}(X) := \text{Tr}_e \rho_W^{\text{init}}(X)$ . Scalar nuclear density  $\rho^{\text{init}}(X)$  is sampled by  $N_{\text{traj}}$  phase space points that serve as initial conditions for  $N_{\text{traj}}$  trajectories propagated using either the LMFD or FSSH dynamics. For each generated phase space point, the electronic part  $\rho_e^{\text{init}}(X)$  satisfies  $\text{Tr}_e \rho_e^{\text{init}}(X) = 1$ . In the case of LMFD,  $X$  determines the initial condition completely. In the case of FSSH, one also needs to select the initial surface randomly for each

trajectory according to the following prescription: For a trajectory starting at  $X$ , the probability for its initial surface to be surface  $j$  is given by the diagonal element  $\rho_{e,j,j}^{\text{init}}(X)$ . Equation (10) for fidelity amplitude is rewritten as

$$f_{\text{MSDR}}(t) = \left\langle \text{Tr}_e \left[ \rho_e^{\text{init}}(X) \cdot \mathcal{T} e^{-i\epsilon \int_0^t \mathbf{V}_W^I(X,t') dt' / \hbar} \right] \right\rangle_{\rho^{\text{init}}(X)}, \quad (28)$$

where we have used the notation

$$\langle A(X) \rangle_{\rho(X)} := \frac{\int dX \rho(X) A(X)}{\int dX \rho(X)}$$

and the fact that  $\langle \text{Tr}_e \rho_e^{\text{init}}(X) \rangle_{\rho^{\text{init}}(X)} = 1$ . The time-ordered product  $\mathcal{T} e^{-i\epsilon \int_0^t \mathbf{V}_W^I(X,t') dt' / \hbar}$  is evaluated along each trajectory by successive multiplication of short time propagators corresponding to each time step. The exponent of each short time propagator is computed using

$$\mathbf{V}_W^I(X,t) = \mathbf{U}^0(X,t)^{-1} \cdot \mathbf{V}_W(X^0(t)) \cdot \mathbf{U}^0(X,t), \quad (29)$$

where

$$\mathbf{U}^0(X,t) = \mathcal{T} e^{-i \int_0^t \mathbf{H}_W^0(X^0(t')) dt' / \hbar}, \quad (30)$$

and  $X^0(t)$  denotes a trajectory of  $\mathbf{H}_W^0$  starting at  $X^0(0) = X$ . Equation (29) can be vaguely interpreted as a combination of a quantum interaction picture for the electrons and a ‘‘classical interaction picture’’ (in which the perturbation is neglected) for the nuclei. Operator  $\mathbf{U}^0(X,t)$  is again computed by successive multiplication of short time propagators along the trajectory. At the end of the dynamics, the weighted phase space average in Eq. (28) is computed as the arithmetic average over all trajectories:

$$f_{\text{MSDR}}(t) = \frac{1}{N_{\text{traj}}} \sum_{N=1}^{N_{\text{traj}}} \text{Tr}_e \left[ \rho_e^{\text{init}}(X_N) \cdot \mathcal{T} \prod_{M=1}^{M_{\text{step}}} e^{-i\epsilon \mathbf{V}_W^I(X_N, M\Delta t) \Delta t / \hbar} \right]. \quad (31)$$

### 2. Initial Hartree product state

The algorithm simplifies slightly when the initial density operator  $\hat{\rho}^{\text{init}}$  is a Hartree product

$$\hat{\rho}^{\text{init}} = \hat{\rho}_N^{\text{init}} \otimes \rho_e^{\text{init}}, \quad (32)$$

where  $\hat{\rho}_N^{\text{init}}$  and  $\rho_e^{\text{init}}$  are the nuclear and electronic density operators, respectively. This Hartree approximation is usually an excellent approximation outside of coupling regions when only one PES is occupied. For initial density in the product form (32),  $\rho_W^{\text{init}}(X) = \rho^{\text{init}}(X) \rho_e^{\text{init}}$ ,

where  $\rho^{\text{init}}(X) = [\rho_N^{\text{init}}]_{\text{W}}(X)$  and  $\rho_e^{\text{init}}$  is independent of  $X$ . Equations (28) and (31) become

$$f_{\text{MSDR}}(t) = \text{Tr}_e \left[ \rho_e^{\text{init}} \cdot \left\langle \mathcal{T} e^{-i\epsilon \int_0^t \mathbf{v}_{\text{W}}^{\text{I}}(X, t') dt' / \hbar} \right\rangle_{\rho^{\text{init}}(X)} \right] \quad (33)$$

and

$$f_{\text{MSDR}}(t) = \text{Tr}_e \left[ \rho_e^{\text{init}} \cdot \frac{1}{N_{\text{traj}}} \sum_{N=1}^{N_{\text{traj}}} \mathcal{T} \prod_{M=1}^{M_{\text{step}}} e^{-i\epsilon \mathbf{v}_{\text{W}}^{\text{I}}(X_N, M\Delta t) \Delta t / \hbar} \right]. \quad (34)$$

### 3. “Electronically pure” initial state

The algorithm simplifies also for “electronically pure” initial states, by which we mean (in the most general sense) states for which the electronic density matrix  $\rho_e^{\text{init}}(X)$  in the product (27) is pure for all  $X$ , i.e., satisfies the condition  $\text{Tr}_e [\rho_e^{\text{init}}(X)^2] = 1$  and can be written as the tensor product

$$\rho_e^{\text{init}}(X) = \mathbf{c}^{\text{init}}(X) \otimes \mathbf{c}^{\text{init}}(X)^\dagger \quad (35)$$

in terms of an initial electronic wave function  $\mathbf{c}^{\text{init}}(X)$ . The generalized electronically pure states include, as a special case, the Hartree product (32) in which the constant electronic matrix  $\rho_e^{\text{init}}$  is pure (while the nuclear factor  $\rho_N^{\text{init}}$  may be mixed). To derive the simplified expression for  $f_{\text{MSDR}}(t)$ , we first rewrite the approximate Wigner transform of the echo operator in Eq. (28) as a product of the electronic evolution operators:

$$\mathcal{T} e^{-i\epsilon \int_0^t \mathbf{v}_{\text{W}}^{\text{I}}(X, t') dt' / \hbar} = \mathbf{U}^0(X, t)^{-1} \cdot \mathbf{U}^\epsilon(X, t), \quad (36)$$

where  $\mathbf{U}^0(X, t)$  was defined in Eq. (30) and, similarly,

$$\mathbf{U}^\epsilon(X, t) = \mathcal{T} e^{-i \int_0^t \mathbf{H}_{\text{W}}^\epsilon(X^0(t')) dt' / \hbar}. \quad (37)$$

Note that the electronic evolution operators  $\mathbf{U}^0(X, t)$  and  $\mathbf{U}^\epsilon(X, t)$  are defined separately for each nuclear trajectory. Using expression (36), we can rewrite the MSDR of fidelity amplitude (28) as

$$f_{\text{MSDR}}(t) = \left\langle \text{Tr}_e \left[ \rho_e^{\text{init}}(X) \cdot \mathbf{U}^0(X, t)^{-1} \cdot \mathbf{U}^\epsilon(X, t) \right] \right\rangle_{\rho^{\text{init}}(X)}. \quad (38)$$

This expression, which is still valid for any initial state, is equivalent to Eq. (28) when either the LMFD or FSSH dynamics is used for propagation.

For electronically pure states (35), Eq. (38) further simplifies into the weighted phase space average

$$f_{\text{MSDR}}(t) = \left\langle \mathbf{c}^0(X, t)^\dagger \cdot \mathbf{c}^\epsilon(X, t) \right\rangle_{\rho^{\text{init}}(X)}, \quad (39)$$

where  $\mathbf{c}^\epsilon(X, t)$  is the wave function with initial condition  $\mathbf{c}^\epsilon(X, 0) = \mathbf{c}^{\text{init}}(X)$  that solves the Schrödinger equation  $\frac{\partial \mathbf{c}^\epsilon(X, t)}{\partial t} = -\frac{i}{\hbar} \mathbf{H}_{\text{W}}^\epsilon(X^0(t)) \cdot \mathbf{c}^\epsilon(X, t)$  for a single discrete electronic degree of freedom in the Lagrangian reference frame given by  $\mathbf{H}_{\text{W}}^0$ . In both propagation algorithms currently used with the MSDR, i.e., the LMFD and FSSH dynamics,  $\mathbf{c}^0(X, t)$  is already available; only  $\mathbf{c}^\epsilon(X, t)$  has to be determined additionally. Expressed explicitly in terms of trajectories, Eq. (39) allows computing the fidelity amplitude simply as

$$f_{\text{MSDR}}(t) = \frac{1}{N_{\text{traj}}} \sum_{N=1}^{N_{\text{traj}}} \mathbf{c}_N^0(X, t)^\dagger \cdot \mathbf{c}_N^\epsilon(X, t). \quad (40)$$

## III. RESULTS

To test the MSDR, we considered several model systems allowing comparison with the exact quantum-mechanical solution in both the diabatic and adiabatic bases. Specifically, we used variants of the three one-dimensional model potentials introduced by Tully<sup>25</sup> and the simple two-level model of photodissociation of NaI.<sup>68–70</sup> The mass in Tully’s models was set to 2000 a.u., approximately corresponding to the mass of the hydrogen atom. The reduced mass in the model of photodissociation of NaI was set to 35480.25 a.u.

The initial density matrix was in all cases a density matrix of a pure state, so  $f_{\text{MSDR}}$  was evaluated using Eq. (40). In Subsections III A and III B, fidelity is used as a quantitative measure of the importance of the diabatic or nonadiabatic couplings on the dynamics. In other words, Hamiltonian  $\hat{\mathbf{H}}^0$  is the diagonal diabatic (Subsec. III A) or adiabatic (Subsec. III B) Hamiltonian and Hamiltonian  $\hat{\mathbf{H}}^\epsilon$  is the full nondiabatic (Subsec. III A) or nonadiabatic (Subsec. III B) Hamiltonian, respectively. If not mentioned otherwise, the dynamics on  $\hat{\mathbf{H}}^0$  uses the LMFD algorithm. Since the PESs of  $\hat{\mathbf{H}}^0$  are decoupled and (with one exception shown in Fig. 3) only one PES is occupied initially, the dynamics reduces to the simpler Born-Oppenheimer classical dynamics of an ensemble of phase space points. In Subsec. III C, more general Hamiltonians and perturbations are studied.

### A. Nondiabaticity of quantum dynamics

In this Subsection, the fidelity criterion of nondiabaticity of the quantum dynamics in the diabatic basis is studied together with the IMSDR and MSDR approximations of fidelity. The IMSDR was already shown to perform well only when the dynamics was close to the diabatic limit.<sup>29</sup> On the other hand, as demonstrated here, MSDR performs well not only in a broader range of problems but also for lower wave packet energies. Comparisons of both methods with numerically exact quantum

fidelity ( $F_{\text{QM}}$ ) in the diabatic basis can be found in Fig. 2. Figure 2 (a) shows results for the single avoided crossing model of Tully.<sup>25</sup> The initial wave packet has high kinetic energy so that the dynamics is fairly close to the diabatic limit. Thus both extensions of the DR work very well;  $F_{\text{MSDR}}$  is almost indistinguishable from  $F_{\text{QM}}$ . Very similar results were obtained for the other model potentials when the wave packet had sufficient energy to cross the coupling region almost diabatically. Figure 2 (b) demonstrates, on the extended coupling model of Tully,<sup>25</sup> that the survival probability  $P_{\text{QM}}$  itself is not always a good indicator of nonadiabaticity of the dynamics. Here,  $F_{\text{QM}}$  decays quickly to zero despite  $P_{\text{QM}}$  staying close to unity. Indeed, the quantum dynamics on  $\hat{\mathbf{H}}^0$  and  $\hat{\mathbf{H}}^\epsilon$  are very different. Both extensions of the DR reproduce the decay of  $F_{\text{QM}}$  very accurately. Using the double avoided crossing model of Tully,<sup>25</sup> Fig. 2 (c) shows that MSDR can accurately reproduce the fidelity behavior even far from the diabatic limit. Not surprisingly, the IMSDR method fails here. For comparison, Fig. 2 (c) also shows two MSDR results obtained by exchanging the roles of  $\hat{\mathbf{H}}^0$  and  $\hat{\mathbf{H}}^\epsilon$ . Since, in contrast to  $\hat{\mathbf{H}}^0$ ,  $\hat{\mathbf{H}}^\epsilon$  is coupled, both the LMFD and FSSH dynamics allow transitions between PESs: both are good approximations of  $F_{\text{QM}}$ . Finally, Fig. 2 (d) demonstrates that because the MSDR is a semiclassical method based on classical trajectories, not permitting tunneling, the method has to be applied with care. In the case shown, far from the diabatic limit, the wave packet on  $\hat{\mathbf{H}}^0$  reflects back from the coupling region. In the MSDR this reflection results in “rephasing” of the trajectories leading to the rise of fidelity back to values close to unity, in disagreement with the quantum result. Even if roles of  $\hat{\mathbf{H}}^0$  and  $\hat{\mathbf{H}}^\epsilon$  are exchanged, problems persist. In the quantum dynamics, a major part of the wave packet on the coupled Hamiltonian  $\hat{\mathbf{H}}^\epsilon$  passes through the coupling region with the aid of diabatic couplings. When the LMFD is used with MSDR, this behavior and associated fidelity decay are captured qualitatively. When the FSSH dynamics is used, the dynamics is exactly identical to the dynamics on the uncoupled Hamiltonian  $\hat{\mathbf{H}}^0$  because all hops in the FSSH algorithm are frustrated. This points out the importance of tunneling in this relatively narrow region of wave packet energies. When the initial kinetic energy is smaller than that shown in Fig. 2 (d), most of the wave packet bounces back even during quantum dynamics on  $\hat{\mathbf{H}}^\epsilon$  and the MSDR fidelity approaches the quantum result. When the energy is somewhat higher, more trajectories pass the barrier (or fewer hops in the FSSH algorithm on  $\hat{\mathbf{H}}^\epsilon$  are frustrated) and as a consequence the MSDR approaches again the quantum result. Note that the relatively good result of the IMSDR is accidental since the method is not expected to work well so far from the diabatic limit.

## B. Nonadiabaticity of quantum dynamics

In this Subsection, the fidelity criterion of nonadiabaticity of the quantum dynamics in the adiabatic basis is studied together with the IMSDR and MSDR approximations of fidelity. As can be seen in Fig. 3, in the adiabatic basis the IMSDR does not work at all, whereas the MSDR works as satisfactorily as in the diabatic basis. Figure 3 (a) shows results for the photodissociation dynamics of NaI close to the adiabatic limit. A low energy wave packet oscillates on the excited adiabatic PES, crossing the coupling region twice per period, each time losing a bit of the excited PES population due to the transition to the ground PES. The MSDR reproduces the associated fidelity decay very well, whereas the IMSDR fails completely. Dynamics even closer to the adiabatic limit is shown in Fig. 3 (b) using Tully’s single avoided crossing model A. First of all, note that  $F_{\text{QM}}$  is again substantially different from the survival probability  $P_{\text{QM}}$ . Second, the figure also shows that in certain cases the MSDR based on the first order nonadiabatic mixed quantum-classical equation [Eq. (13)] does not accurately reproduce  $F_{\text{QM}}$ . Interestingly, the agreement can be improved with the second order dynamics, which employs the complete partially Wigner transformed nonadiabatic Hamiltonian

$$\mathbf{H}_{\text{W}}^{\text{A,comp}} = \mathbf{H}_{\text{W}}^{\text{A}} - i\hbar \frac{P}{M} \mathbf{F} - \frac{\hbar^2}{2M} \mathbf{F} \cdot \mathbf{F}. \quad (41)$$

Strictly speaking such an approach goes beyond the MSDR defined by Eqs. (10) and (13). Nevertheless, in the special case of a decoupled unperturbed Hamiltonian  $\hat{\mathbf{H}}^0$  with only one occupied PES, the second order equation of motion can be easily used instead of Eq. (13), because the increased order of dynamics affects only phases. Trajectories, which are propagated with the decoupled Hamiltonian  $\hat{\mathbf{H}}^0$ , stay unaffected since the contribution from the second order Poisson brackets vanishes. The second-order Hamiltonian (41), however, cannot be derived by generalizing the approach used to derive Eq. (26). In that case, the mixed quantum-classical equation (13) was derived from the Liouville-Von Neumann equation in the diabatic basis and then transformed into the adiabatic basis using Eq. (24) to yield Eq. (26). Generalizing this approach to the second order, no correction is obtained to the first order Hamiltonian acting on the electronic degree of freedom in the Lagrangian frame. Instead, we have used a generalization to the second order of the approach from Ref. 18, where the mixed quantum-classical equation was obtained directly by Wigner transforming the Liouville-Von Neumann equation expressed in the adiabatic basis. The exact reason for the discrepancy between the two approaches is not yet clear to us and will be a subject of further investigation. (Some discrepancy is actually present already in the first order.) In other examples that we have studied, the second order correction does not significantly influence the results. Finally, Fig. 3 (b) also demonstrates the convergence of the MSDR with the number of trajectories showing that



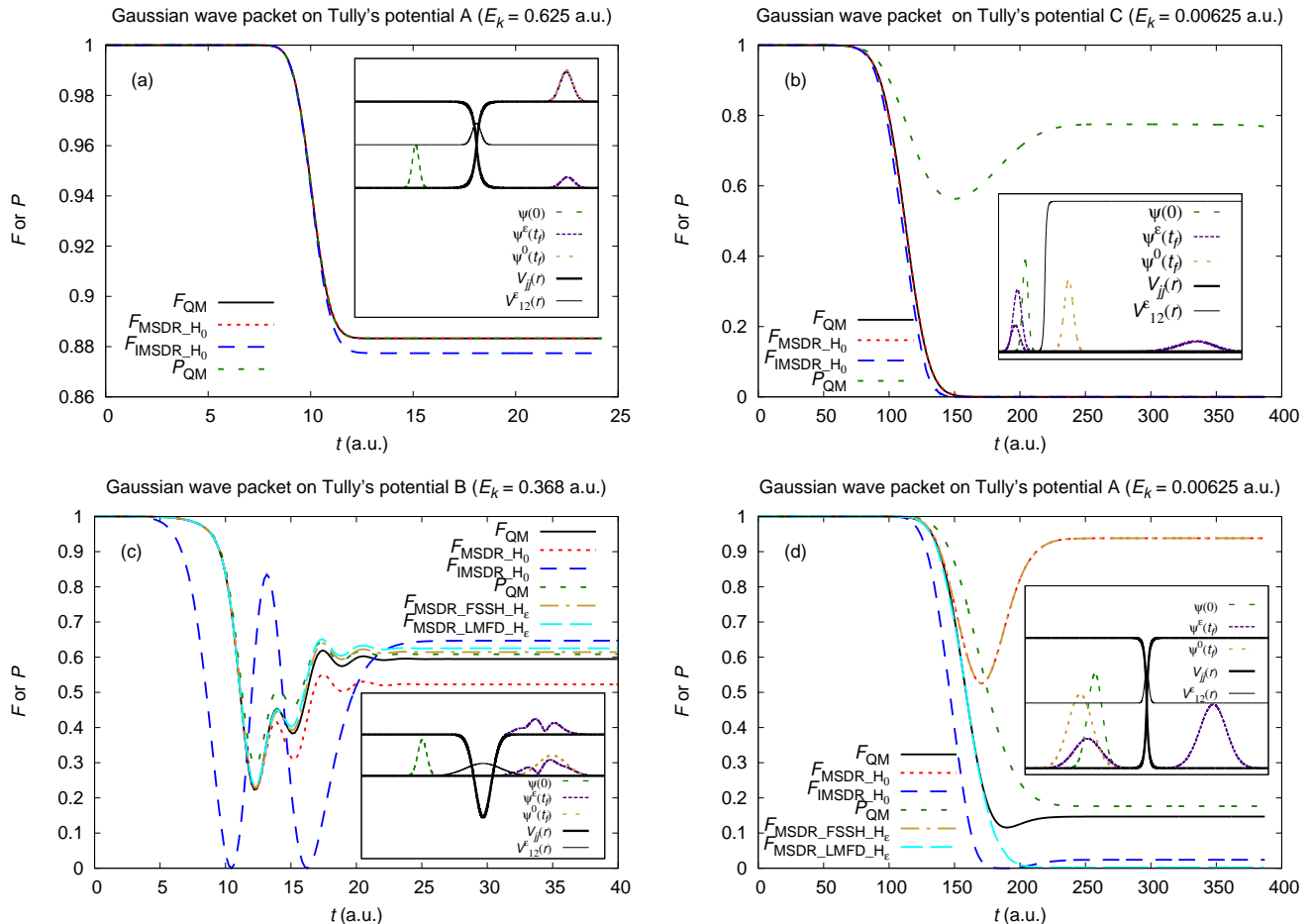


Figure 2. Nondiabaticity of quantum dynamics. Panels (a)-(d) compare the numerically exact quantum fidelity ( $F_{QM}$ ) with extensions of the DR in the diabatic basis and with the quantum survival probability ( $P_{QM}$ ). (a) Dynamics close to the diabatic limit. (b) Dynamics very far from the diabatic limit. (c) Dynamics in the intermediate range. (d) Dynamics in the region where quantum tunneling is important. The insets show the diabatic PESs  $V_{jj}(r)$ , diabatic coupling  $V_{12}(r)$  as well as initial  $[\psi(0)]$  and final  $[\psi^0(t_f)$  and  $\psi^\epsilon(t_f)]$  wave functions evolved with  $\hat{H}^0$  and  $\hat{H}^\epsilon$ , respectively.

as few as 32 trajectories suffice for an accurate approximation of  $F_{QM}$ . (The convergence is similar for both the first order and the second order dynamics.) For the DR<sup>43,54</sup> and IMSDR,<sup>29</sup> an exact formula exists for the number of trajectories as a function of the statistical error and of fidelity. For the MSDR, such an exact formula has not been derived, but similarly to the DR<sup>43,54</sup> and IMSDR,<sup>29</sup> more trajectories have to be used for lower fidelity. Figure 3 (c) shows that the MSDR usually retains its accuracy even far from the adiabatic limit. Nevertheless, similarly to the diabatic basis, special care should be taken in such cases.

In all examples discussed above, only one PES was occupied initially. Yet the MSDR works also with more general initial conditions, as shown in Fig. 3 (d) using Tully's single avoided crossing model. Here 75 % of the initial density is located on the lower PES, and the rest on the upper one. Note that when more than one PES of  $\hat{H}^0$  is occupied, one must watch out for the intrinsic deficiencies

of the underlying dynamical methods. If the LMFD is used for propagation (not shown), each trajectory propagates on an average PES, given by the weighted average of all occupied PES, even outside of coupling regions. When the FSSH based algorithm is used [as shown in Fig. 3 (d)], other problems may occur in a similar situation, i.e., when wave packet dynamics on the lower and upper PESs differ substantially outside of coupling regions.

### C. Importance of an additional interaction in the Hamiltonian and accuracy of an approximate Hamiltonian

Now we consider two more general applications of the MSDR. In the first application, the MSDR is used to evaluate the importance of an additional interaction term in the Hamiltonian. In the second application, the method

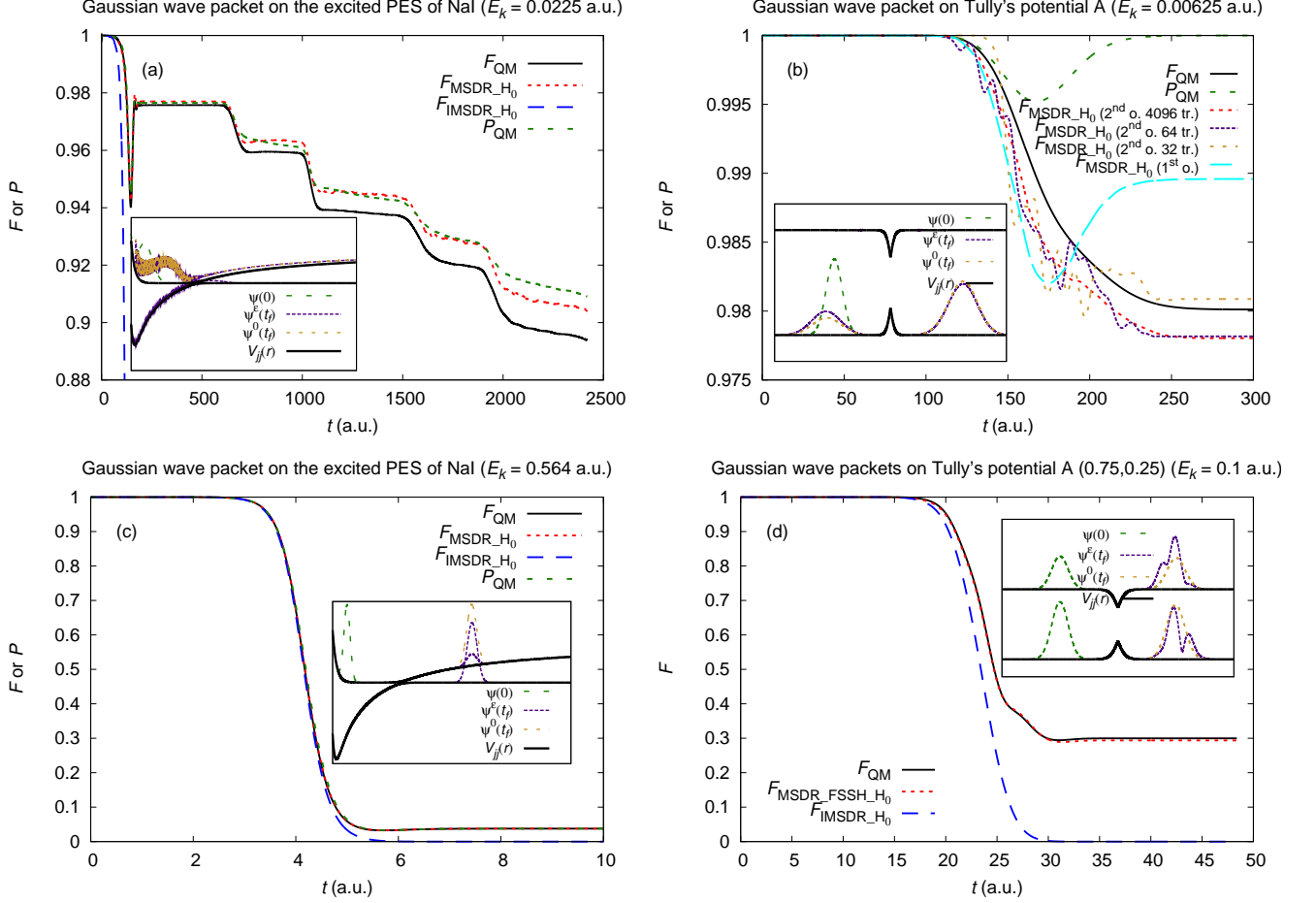


Figure 3. Nonadiabaticity of quantum dynamics. Panels (a)-(d) compare the numerically exact quantum fidelity ( $F_{\text{QM}}$ ) with the extensions of the DR in the adiabatic basis and (when applicable) with the quantum survival probability ( $P_{\text{QM}}$ ). (a) Dynamics close to the adiabatic limit. (b) Convergence of the MSDR and importance of the second order dynamics close to the adiabatic limit. (c) Dynamics very far from the adiabatic limit. (d) A more general initial condition with both PESs initially occupied. The insets show the adiabatic PESs  $V_{jj}(r)$  as well as initial  $[\psi(0)]$  and final  $[\psi^o(t_f)$  and  $\psi^e(t_f)]$  wave functions evolved with  $\hat{\mathbf{H}}^0$  and  $\hat{\mathbf{H}}^\epsilon$ , respectively.

is employed to evaluate the accuracy of quantum dynamics on an approximate non(a)diabatic Hamiltonian. In both cases,  $\hat{\mathbf{H}}^0$  and  $\hat{\mathbf{H}}^\epsilon$  are coupled and may differ in both diagonal and coupling terms. Because even  $\hat{\mathbf{H}}^0$  is coupled, the trajectories used in the MSDR do not anymore correspond to simpler Born-Oppenheimer trajectories even when only one PES is occupied initially.

### 1. Importance of an additional interaction in the Hamiltonian

The importance of an additional interaction in the Hamiltonian is tested in Fig. 4(a). This case is similar to previously studied problems because  $\hat{\mathbf{H}}^0$  and  $\hat{\mathbf{H}}^\epsilon$  differ again only by the presence of a coupling element; the difference is that  $\hat{\mathbf{H}}^0$  is now coupled. Both diabatic Hamiltonians contain three PESs, of which the lower two

are identical to the PESs of Tully's single avoided crossing model. The third PES is flat with constant energy  $E = 0.15$  a.u. In both Hamiltonians, the lower two PESs are coupled by the same coupling term  $V_{12}$  as in the original single avoided crossing model. Additionally, in  $\hat{\mathbf{H}}^\epsilon$  (but not in  $\hat{\mathbf{H}}^0$ ), the highest two PESs are coupled with

$$V_{23} = V_{32}^* = (1 + i) [C \exp(-DQ^2)], \quad (42)$$

where  $C = 0.005$  and  $D = 1.0$ . A more general complex form was chosen to emulate the presence of spin-orbit coupling terms, which may also be complex valued. As can be seen from the figure, the MSDR reproduces the exact decay of fidelity accurately. Note that fidelity decays significantly even though only approximately 1 % of the probability density ends up on the highest PES. In other words, this is yet another example, where the survival probability is a poor measure of the importance of couplings between PESs.

## 2. Accuracy of an approximate Hamiltonian

The last application of the MSDR that we consider is the evaluation of the accuracy of an approximate Hamiltonian. An additional difficulty related to this application is that the electronic basis sets used to represent the two Hamiltonians may be different. In the adiabatic basis set, electronic basis functions are determined at each space point by the Hamiltonian itself. The diabatic basis, on the other hand, is usually chosen to diagonalize the Hamiltonian at some fixed nuclear configuration. To avoid difficulties, one may express both Hamiltonians in the same basis set, but this is not always feasible (at least not easily). Such problem occur, e.g., when one compares two Hamiltonians computed on the fly using different electronic structure methods. Since Hamiltonians used in electronic structure methods are usually approximate, the adiabatic basis functions are not necessarily identical. Moreover, in some methods, such as DFT, electronic basis functions do not even have to be determined. Therefore, as we are interested in the dynamics of nuclei and in the extent of electronic transitions rather than in approximations underlying electronic structure methods, we solve this problem by replacing our definition of fidelity  $F_{\text{QM}}$  with an alternative definition  $F'_{\text{QM}}$ , in which the overlap matrix of electronic basis functions is always assumed to be the identity matrix.

An “approximate” Hamiltonian  $\hat{H}^\epsilon$  was created by perturbing one of the parameters in the analytical formula for  $\hat{H}^0$  in the diabatic basis. (The perturbation was transformed into the adiabatic basis when the dynamics was done in the adiabatic basis). First, the effect of perturbing the slope of PESs in the coupling region was studied using Tully’s single avoided crossing model in the diabatic basis [see Fig. 4 (b)]. The perturbation consisted in increasing the value of parameter  $B$  in Eq. (21) in Ref. 25 by 50%. Although electronic transitions are significant even on  $\hat{H}^0$  itself, the MSDR works very well with both the LMFD and FSSH dynamics. Figure 4 (c) shows the decay of fidelity due to an increased depth of the PES well in Tully’s double avoided crossing model. Calculations were performed both in the diabatic and adiabatic basis. [Note that  $F'_{\text{QM}}$  may differ between adiabatic and diabatic basis, but only in coupling regions. In the case shown in Fig. 4 (c) the difference is not significant.] To increase the depth of the well in  $\hat{H}^\epsilon$ , value of parameter  $A$  in Eq. (23) in Ref. 25 was increased by 10 %. As can be seen in Fig. 4 (c), the quantum result is reproduced very well by the MSDR based on the LMFD in both basis sets. When the FSSH dynamics is used, the result depends strongly on the basis. In the adiabatic basis, the MSDR reproduces the quantum result quite well, whereas in the diabatic basis, the method fails to follow  $F'_{\text{QM}}$  even qualitatively. Worse performance of the FSSH dynamics in the diabatic basis is well known,<sup>71</sup> and in this specific case may be attributed mainly to the fact that 40% of hops in the diabatic basis are frustrated.

Figure 4 (d) shows an opposite case, where the MSDR

works better with the FSSH than with LMFD. The model used is Tully’s extended coupling model in the adiabatic basis. To introduce the perturbation, the coupling strength in  $\hat{H}^\epsilon$  (parameter  $B$  in Eq. (24) in Ref. 25) was increased by 50%. The MSDR reproduces the initial decay of fidelity irrespective of the dynamics used. By contrast, the subsequent rise of fidelity caused by the partial reflection of the wave packet could be reproduced only with the FSSH dynamics because no reflection occurs in the mean field description.

## D. Computational details

All quantum calculations in the diabatic basis set were performed using the second order split-operator algorithm.<sup>72</sup> Calculations in the adiabatic basis were done either by transforming the quantum state into the diabatic basis, propagating there, and transforming back into the adiabatic basis, or directly with the second order Fourier method.<sup>73</sup> The LMFD or FSSH dynamics were done using the second order symplectic Verlet integrator.<sup>74</sup>

## IV. DISCUSSION AND CONCLUSIONS

Results presented above demonstrate that quantum fidelity is useful as a quantitative measure of nonadiabaticity or nonadiabaticity of quantum dynamics. Moreover the MSDR, a semiclassical approximation developed in this work, has proven to be a reliable yet very efficient substitute for the expensive exact quantum dynamics calculation of fidelity. The MSDR, similarly to the less accurate IMSDR,<sup>29</sup> is a generalization of DR to non(a)diabatic dynamics. In addition to quantum effects originating from the interaction of nuclei with electrons, which are included in most mixed quantum-classical methods, the MSDR includes also quantum effects originating from the interference between mixed quantum-classical trajectories representing the evolution of the initial density matrix. Two approximate variants of the MSDR were developed and studied numerically: the former uses the LMFD, derived here, while the latter employs the FSSH dynamics. The LMFD, although obtained in a different way, is equivalent to the nuclear dynamics appearing in the nonadiabatic IVR,<sup>14,65,75</sup> which is, in turn, nothing else than the Ehrenfest dynamics applied separately to each classical phase space point representing the initial density matrix. Both FSSH and the Ehrenfest method are relatively simple and often used, thus both variants of MSDR can be easily implemented into any FSSH or Ehrenfest dynamics code, especially for pure states.

Several applications of the MSDR in nonadiabatic dynamics were presented. First, the method was used to approximate a rigorous quantitative measure of nonadiabaticity or nonadiabaticity of the dynamics based on

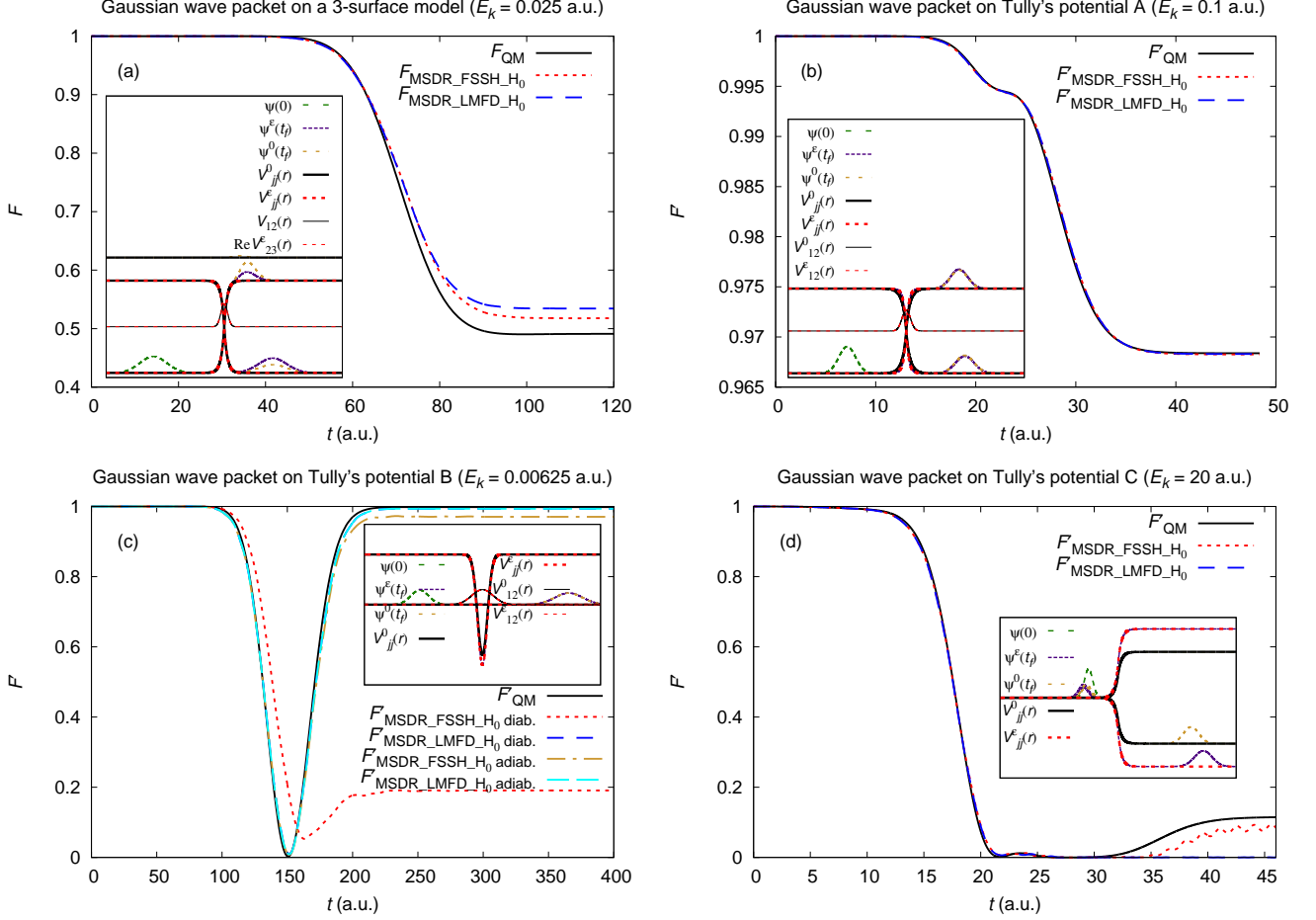


Figure 4. (a) Fidelity as a measure of the effects of additional (e.g., spin-orbit) couplings on the quantum dynamics. (b)-(d) Fidelity as a measure of the accuracy of quantum dynamics on an approximate Hamiltonian. Comparison of the numerically exact quantum fidelity ( $F_{\text{QM}}$  or  $F'_{\text{QM}}$ ) with extensions of the DR. The insets show the diabatic or adiabatic PESs  $V_{jj}(r)$ , diabatic couplings  $V_{12}(r)$  and  $V_{23}(r)$  as well as the initial  $[\psi(0)]$  and final  $[\psi^0(t_f)$  and  $\psi^\epsilon(t_f)]$  wave functions evolved with  $\hat{\mathbf{H}}^0$  and  $\hat{\mathbf{H}}^\epsilon$ , respectively.

quantum fidelity. As such the MSDR may be used to decide - before running the quantum dynamics itself - which PESs or Hamiltonian terms are important. Second, the method permits establishing the relative importance of several interaction terms in a Hamiltonian. Third, generalizing one of the applications of the original DR,<sup>39,40</sup> the MSDR may be used to evaluate the accuracy of quantum dynamics with an approximate non(a)diabatic Hamiltonian. Apart from these applications, the MSDR could be used, in principle, to compute all quantities expressible in terms of quantum fidelity or quantum fidelity amplitude, such as various spectra.

In Section III we have demonstrated that for one dimensional model systems the MSDR works often satisfactorily even far from the diabatic or adiabatic limit. The method has yet to be tested in multi-dimensional systems. Nevertheless, results obtained with the original Born-Oppenheimer DR method demonstrate that the convergence of the method is actually independent of the

dimensionality of a problem<sup>54</sup> and that the accuracy does not deteriorate with dimensionality.<sup>39</sup> Thus, we expect that the MSDR would perform well especially in chaotic multi-dimensional systems such as some molecules, provided that the underlying mixed classical-quantum dynamics is a reasonable approximation to the quantum dynamics. Unfortunately, this is not always the case. It is well known that the Ehrenfest dynamics (and also the LMFD) can be qualitatively incorrect when coupling vanishes after passing a coupling region and more PESs are occupied. In the MSDR this problem is often less significant, because in many cases after passing the coupling region fidelity does not decay anymore. The FSSH dynamics also suffers from several problems besides the inaccuracies caused by the classical description of nuclei, such as the problem of “excessive coherence” related (similarly as for the LMFD) to the fact that all matrix elements of the density matrix attached to a trajectory evolve on the same PES. In many cases, this can be al-

leviated by applying the “decoherence” correction.<sup>76–80</sup> Including a similar correction into the MSDR method should be straightforward and will be explored in future work. Another possibility how to overcome some deficiencies of the LMFD or FSSH dynamics would be to use the MSDR together with one of the propagation meth-

ods attempting to solve the mixed quantum-classical Liouville equation directly.

#### Acknowledgement

This research was supported by the Swiss NSF NCCR MUST (Molecular Ultrafast Science & Technology) and by the EPFL.

- 
- \* jiri.vanicek@epfl.ch
- <sup>1</sup> L. J. Butler, *Annu. Rev. Phys. Chem.* **49**, 125 (1998).
  - <sup>2</sup> G. A. Worth and L. S. Cederbaum, *Annu. Rev. Phys. Chem.* **55**, 127 (2004).
  - <sup>3</sup> M. S. Child and M. A. Robb, eds., *Non-Adiabatic Effects in Chemical Dynamics*, vol. 127 of *Faraday Discussions* (Royal Society of Chemistry, Cambridge, UK, 2004).
  - <sup>4</sup> H.-D. Meyer, F. Gatti, and G. A. Worth, eds., *Multidimensional Quantum Dynamics: MCTDH Theory and Applications* (Wiley-VCH, Weinheim, 2009).
  - <sup>5</sup> M. Eroms, M. Jungen, and H.-D. Meyer, *J. Phys. Chem. A* **114**, 9893 (2010).
  - <sup>6</sup> R. E. Wyatt, C. L. Lopreore, and G. Parlant, *J. Chem. Phys.* **114**, 5113 (2001).
  - <sup>7</sup> C. L. Lopreore and R. E. Wyatt, *J. Chem. Phys.* **116**, 1228 (2002).
  - <sup>8</sup> B. F. E. Curchod, I. Tavernelli, and U. Rothlisberger, *Phys. Chem. Chem. Phys.* **13**, 3231 (2011).
  - <sup>9</sup> T. J. Martínez, M. Ben-Nun, and R. D. Levine, *J. Phys. Chem.* **100**, 7884 (1996).
  - <sup>10</sup> S. Yang, J. D. Coe, B. Kaduk, and T. J. Martínez, *J. Chem. Phys.* **130**, 134113 (2009).
  - <sup>11</sup> J. C. Burant and V. S. Batista, *J. Chem. Phys.* **116**, 2748 (2002).
  - <sup>12</sup> A. Kondorskiy and H. Nakamura, *J. Chem. Phys.* **120**, 8937 (2004).
  - <sup>13</sup> Y. Wu and M. F. Herman, *J. Chem. Phys.* **123**, 144106 (2005).
  - <sup>14</sup> W. H. Miller, *J. Phys. Chem. A* **113**, 1405 (2009).
  - <sup>15</sup> E. J. Heller, B. Segev, and A. V. Sergeev, *J. Phys. Chem. B* **106**, 8471 (2002).
  - <sup>16</sup> A. Donoso and C. C. Martens, *J. Phys. Chem. A* **102**, 4291 (1998).
  - <sup>17</sup> R. Kapral and G. Ciccotti, *J. Chem. Phys.* **110**, 8919 (1999).
  - <sup>18</sup> I. Horenko, C. Salzmann, B. Schmidt, and C. Schütte, *J. Chem. Phys.* **117**, 11075 (2002).
  - <sup>19</sup> K. Ando and M. Santer, *J. Chem. Phys.* **118**, 10399 (2003).
  - <sup>20</sup> I. Horenko, M. Weiser, B. Schmidt, and C. Schütte, *J. Chem. Phys.* **120**, 8913 (2004).
  - <sup>21</sup> D. A. Micha and B. Thorndyke, in *A Tribute Volume in Honor of Professor Osvaldo Goscinski*, edited by E. Brandas and E. Brandas (Academic Press, 2004), vol. 47 of *Advances in Quantum Chemistry*, pp. 293 – 314.
  - <sup>22</sup> D. Mac Kernan, G. Ciccotti, and R. Kapral, *J. Phys. Chem. B* **112**, 424 (2008).
  - <sup>23</sup> S. Bonella, G. Ciccotti, and R. Kapral, *Chem. Phys. Lett.* **484**, 399 (2010).
  - <sup>24</sup> D. Bousquet, K. H. Hughes, D. A. Micha, and I. Burghardt, *J. Chem. Phys.* **134**, 064116 (2011).
  - <sup>25</sup> J. C. Tully, *J. Chem. Phys.* **93**, 1061 (1990).
  - <sup>26</sup> S. Nielsen, R. Kapral, and G. Ciccotti, *J. Stat. Phys.* **101**, 225 (2000).
  - <sup>27</sup> N. Shenvi, *J. Chem. Phys.* **130**, 124117 (2009).
  - <sup>28</sup> E. R. Dunkel, S. Bonella, and D. F. Coker, *J. Chem. Phys.* **129**, 114106 (2008).
  - <sup>29</sup> T. Zimmermann and J. Vaníček, *J. Chem. Phys.* **132**, 241101 (2010).
  - <sup>30</sup> H. Tao, B. G. Levine, and T. J. Martínez, *J. Phys. Chem. A* **113**, 13656 (2009).
  - <sup>31</sup> H. Frauenfelder and P. G. Wolynes, *Science* **229**, 337 (1985).
  - <sup>32</sup> L. D. Landau, *Phys. Z. Sowjetunion* **1**, 88 (1932).
  - <sup>33</sup> L. D. Landau, *Phys. Z. Sowjetunion* **2**, 46 (1932).
  - <sup>34</sup> C. Zener, *Proc. R. Soc. London A* **137**, 696 (1932).
  - <sup>35</sup> E. C. G. Stückelberg, *Helv. Phys. Acta* **5**, 369 (1932).
  - <sup>36</sup> E. E. Nikitin, *Annu. Rev. Phys. Chem.* **50**, 1 (1999).
  - <sup>37</sup> A. Peres, *Phys. Rev. A* **30**, 1610 (1984).
  - <sup>38</sup> R. MacKenzie, M. Pineault, and L. Renaud-Desjardins, arXiv:1109.2565v1 (2011).
  - <sup>39</sup> B. Li, C. Mollica, and J. Vaníček, *J. Chem. Phys.* **131**, 041101 (2009).
  - <sup>40</sup> T. Zimmermann, J. Ruppen, B. Li, and J. Vaníček, *Int. J. Quantum Chem.* **110**, 2426 (2010).
  - <sup>41</sup> J. Vaníček and E. J. Heller, *Phys. Rev. E* **68**, 056208 (2003).
  - <sup>42</sup> J. Vaníček, *Phys. Rev. E* **70**, 055201 (2004).
  - <sup>43</sup> J. Vaníček, *Phys. Rev. E* **73**, 046204 (2006).
  - <sup>44</sup> L. M. Hubbard and W. H. Miller, *J. Chem. Phys.* **78**, 1801 (1983).
  - <sup>45</sup> S. Mukamel, *J. Chem. Phys.* **77**, 173 (1982).
  - <sup>46</sup> J. M. Rost, *J. Phys. B* **28**, L601 (1995).
  - <sup>47</sup> Z. Li, J.-Y. Fang, and C. C. Martens, *J. Chem. Phys.* **104**, 6919 (1996).
  - <sup>48</sup> S. A. Egorov, E. Rabani, and B. J. Berne, *J. Chem. Phys.* **108**, 1407 (1998).
  - <sup>49</sup> Q. Shi and E. Geva, *J. Chem. Phys.* **122**, 064506 (2005).
  - <sup>50</sup> M. Wehrle, M. Šulc, and J. Vaníček, *Chimia* **65**, 334 (2011).
  - <sup>51</sup> T. Gorin, T. Prosen, T. H. Seligman, and M. Znidaric, *Physics Reports* **435**, 33 (2006).
  - <sup>52</sup> D. A. Wisniacki, N. Ares, and E. G. Vergini, *Phys. Rev. Lett.* **104**, 254101 (2010).
  - <sup>53</sup> I. García-Mata, R. O. Vallejos, and D. A. Wisniacki, arXiv:1106.4206.
  - <sup>54</sup> C. Mollica and J. Vaníček, *Phys. Rev. Lett.* **107**, 214101 (2011).
  - <sup>55</sup> M. Ceotto, S. Atahan, G. F. Tantardini, and A. Aspuru-Guzik, *J. Chem. Phys.* **130**, 234113 (2009).
  - <sup>56</sup> G. Veble and T. Prosen, *Phys. Rev. Lett.* **92**, 034101 (2004).
  - <sup>57</sup> E. Wigner, *Phys. Rev.* **40**, 749 (1932).
  - <sup>58</sup> I. V. Aleksandrov, *Zeitschrift Fur Naturforschung Section A-a Journal of Physical Sciences* **36**, 902 (1981).
  - <sup>59</sup> W. Boucher and J. Traschen, *Phys. Rev. D* **37**, 3522 (1988).

- <sup>60</sup> C. C. Martens and J. Y. Fang, *J. Chem. Phys.* **106**, 4918 (1997).
- <sup>61</sup> O. V. Prezhdo and V. V. Kisil, *Phys. Rev. A* **56**, 162 (1997).
- <sup>62</sup> J. Caro and L. L. Salcedo, *Phys. Rev. A* **60**, 842 (1999).
- <sup>63</sup> Q. Shi and E. Geva, *J. Chem. Phys.* **121**, 3393 (2004).
- <sup>64</sup> R. Grunwald, A. Kelly, and R. Kapral, in *Energy Transfer Dynamics in Biomaterial Systems*, edited by I. Burghardt, V. May, D. A. Micha, E. R. Bittner, F. Schäfer, J. Toennies, and W. Zinth (Springer Berlin Heidelberg, 2009), vol. 93 of *Springer Series in Chemical Physics*, pp. 383–413, ISBN 978-3-642-02306-4.
- <sup>65</sup> N. Ananth, C. Venkataraman, and W. H. Miller, *J. Chem. Phys.* **127**, 084114 (2007).
- <sup>66</sup> H.-D. Meyer and W. H. Miller, *J. Chem. Phys.* **70**, 3214 (1979).
- <sup>67</sup> G. Stock and M. Thoss, *Phys. Rev. Lett.* **78**, 578 (1997).
- <sup>68</sup> V. Engel and H. Metiu, *J. Chem. Phys.* **90**, 6116 (1989).
- <sup>69</sup> N. van Veen, M. D. Vries, J. Sokol, T. Baller, and A. de Vries, *Chem. Phys.* **56**, 81 (1981).
- <sup>70</sup> M. B. Faist and R. D. Levine, *J. Chem. Phys.* **64**, 2953 (1976).
- <sup>71</sup> J. C. Tully, *Faraday Discuss.* **110**, 407 (1998).
- <sup>72</sup> M. D. Feit and J. A. Fleck, Jr., *J. Chem. Phys.* **78**, 301 (1983).
- <sup>73</sup> D. Kosloff and R. Kosloff, *J. Comput. Phys.* **52**, 35 (1983).
- <sup>74</sup> L. Verlet, *Phys. Rev.* **159**, 98 (1967).
- <sup>75</sup> X. Sun and W. H. Miller, *J. Chem. Phys.* **106**, 6346 (1997).
- <sup>76</sup> J.-Y. Fang and S. Hammes-Schiffer, *J. Phys. Chem. A* **103**, 9399 (1999).
- <sup>77</sup> C. Y. Zhu, S. Nangia, A. W. Jasper, and D. G. Truhlar, *J. Chem. Phys.* **121**, 7658 (2004).
- <sup>78</sup> G. Granucci and M. Persico, *J. Chem. Phys.* **126**, 134114 (2007).
- <sup>79</sup> G. Granucci, M. Persico, and A. Zocante, *J. Chem. Phys.* **133**, 134111 (2010).
- <sup>80</sup> J. E. Subotnik and N. Shenoi, *J. Chem. Phys.* **134**, 024105 (2011).